

Potassium Currents in Octopus Cells of the Mammalian Cochlear Nucleus

RAMAZAN BAL AND DONATA OERTEL

Department of Physiology, University of Wisconsin, Madison, Wisconsin 53706

Received 7 March 2001; accepted in final form 2 July 2001

Bal, Ramazan and Donata Oertel. Potassium currents in octopus cells of the mammalian cochlear nucleus. *J Neurophysiol* 86: 2299–2311, 2001. Octopus cells in the posteroventral cochlear nucleus (PVCN) of mammals are biophysically specialized to detect coincident firing in the population of auditory nerve fibers that provide their synaptic input and to convey its occurrence with temporal precision. The precision in the timing of action potentials depends on the low input resistance ($\sim 6\text{ M}\Omega$) of octopus cells at the resting potential that makes voltage changes rapid ($\tau \sim 200\ \mu\text{s}$). It is the activation of voltage-dependent conductances that endows octopus cells with low input resistances and prevents repetitive firing in response to depolarization. These conductances have been examined under whole cell voltage clamp. The present study reveals the properties of two conductances that mediate currents whose reversal at or near the equilibrium potential for K^+ over a wide range of extracellular K^+ concentrations identifies them as K^+ currents. One rapidly inactivating conductance, g_{KL} , had a threshold of activation at -70 mV , rose steeply as a function of depolarization with half-maximal activation at $-45 \pm 6\text{ mV}$ (mean \pm SD), and was fully activated at 0 mV . The low-threshold K^+ current (I_{KL}) was largely blocked by α -dendrotoxin (α -DTX) and partially blocked by DTX-K and tityus-toxin, indicating that this current was mediated through potassium channels of the Kv1 (also known as *shaker* or KCNA) family. The maximum low-threshold K^+ conductance (g_{KL}) was large, $514 \pm 135\text{ nS}$. Blocking I_{KL} with α -DTX revealed a second K^+ current with a higher threshold (I_{KH}) that was largely blocked by 20 mM tetraethylammonium (TEA). The more slowly inactivating conductance, g_{KH} , had a threshold for activation at -40 mV , reached half-maximal activation at $-16 \pm 5\text{ mV}$, and was fully activated at $+30\text{ mV}$. The maximum high-threshold conductance, g_{KH} , was on average $116 \pm 27\text{ nS}$. The present experiments show that it is not the biophysical and pharmacological properties but the magnitude of the K^+ conductances that make octopus cells unusual. At the resting potential, -62 mV , g_{KL} contributes $\sim 42\text{ nS}$ to the resting conductance and mediates a resting K^+ current of 1 nA . The resting outward K^+ current is balanced by an inward current through the hyperpolarization-activated conductance, g_{h} , that has been described previously.

INTRODUCTION

The low input resistance of octopus cells causes synaptic responses to be brief and voltage changes in response to synaptic current to be small. Octopus cells require the summation of many synaptic inputs within a period of 1 ms to fire and thus detect coincident firing among their inputs (Golding et al. 1995). In requiring the summation of many small inputs to

produce a brief but robust synaptic response, the temporal jitter in the timing of individual auditory nerve inputs is lost in the firing of octopus cells. In vivo octopus cells convey the timing of broadband transients or periodicity in sounds with a temporal jitter $< 200\ \mu\text{s}$ (Godfrey et al. 1975; Oertel et al. 2000; Rhode and Smith 1986; Rhode et al. 1983). Octopus cells can fire at rates ≤ 800 action potentials/s (Rhode and Smith 1986). Tones typically evoke a single, sharply timed action potential at the onset of the stimulus; in responses to tones $< 800\text{ Hz}$, octopus cells can fire at every cycle (Friauf and Ostwald 1988; Godfrey et al. 1975; Rhode and Smith 1986; Smith et al. 1993).

Octopus cells have been recognized in all mammals including humans (Adams 1986; Hackney et al. 1990; Osen 1969; Willard and Martin 1983; Willott and Bross 1990). They occupy the octopus cell area, a region that is defined by a clear border in the caudal and dorsal part of the PVCN (Kolston et al. 1992; Wickesberg et al. 1994; Willott and Bross 1990). Their axons form one of the ascending pathways through the brain stem. They project contralaterally through the intermediate acoustic stria to excite neurons in the superior paraolivary nucleus (SPN) and in the ventral nucleus of the lateral lemniscus (VNLL) (Adams 1997; Schofield 1995; Schofield and Cant 1997; Smith et al. 1993; Vater et al. 1997; Warr 1969). The influence of octopus cells on the inferior colliculus is indirect and inhibitory as neurons in the SPN are GABAergic (Kulesza and Berrebi 1999) and neurons in the VNLL that are innervated by octopus cells are glycinergic (Saint Marie et al. 1997). It has been suggested that these pathways play a role in the recognition of temporal patterns in natural sounds.

Several conductances contribute to the low input resistance of octopus cells. In the initial studies of octopus cells made with sharp electrodes in current-clamp experiments, it was not possible to measure the input resistance but the dramatic increase of the input resistance in the hyperpolarizing voltage range in the presence of Cs^+ was the first clue that a hyperpolarization-activated conductance contributed to the resting properties of octopus cells (Golding et al. 1995). Recordings with patch-clamp electrodes showed that octopus cells have input resistances of $\sim 6\text{ M}\Omega$ (Bal and Oertel 2000; Golding et al. 1999). The pharmacological sensitivity to 4-aminopyridine (4-AP) (Golding et al. 1999) and to α -DTX (M. Ferragamo and D. Oertel, unpublished results) indicated that a low-threshold K^+ conductance balanced the hyperpolarization-activated con-

Address for reprint requests: D. Oertel, Dept. of Physiology, University of Wisconsin Medical School, 1300 University Ave., Madison, WI 53706 (E-mail: oertel@physiology.wisc.edu).

The costs of publication of this article were defrayed in part by the payment of page charges. The article must therefore be hereby marked "advertisement" in accordance with 18 U.S.C. Section 1734 solely to indicate this fact.

ductance at rest and played a role in shaping the voltage changes produced by synaptic currents. To understand the properties of these conductances, they were examined under voltage clamp. The large amplitude and relatively depolarized voltage range of activation allows the hyperpolarization-activated, mixed-cation conductance, g_h , to contribute to the shaping of synaptic responses and to contribute a large steady current at the resting potential (Bal and Oertel 2000). The present study describes K^+ conductances, one of which balances g_h .

METHODS

Coronal slices of the PVCN from mice (ICR strain) of between 17 and 20 postnatal days were used for these experiments. After decapitation, the head was immersed in normal physiological saline containing (in mM) 130 NaCl, 3 KCl, 1.2 KH_2PO_4 , 2.4 $CaCl_2$, 1.3 $MgSO_4$, 20 $NaHCO_3$, 3 HEPES, and 10 glucose, saturated with 95% O_2 -5% CO_2 , pH 7.4, between 25 and 31°C (Golding et al. 1995, 1999). After the brain was removed from the skull, it was cut coronally at the midcollicular level. The rostral surface of the specimen was mounted on a Teflon block with a cyanoacrylate glue (Superglue). Two slices, 180 μm thick, were then cut using an oscillating tissue slicer (Frederick Haer, New Brunswick, ME). These were transferred to a storage chamber containing fresh, oxygenated saline at 33°C for ≤ 2 h. The slices were transferred to a recording chamber of ~ 0.3 ml in which it was continuously perfused at about 6 ml/min with oxygenated saline whose temperature was kept at 33°C with a custom-made, feedback-controlled heater.

Slices were visualized with a Zeiss Axioskop with a $\times 63$ water-immersion lens. Octopus cells were initially identified by their characteristic location within a heavily myelinated fiber bundle just ventral and caudal to the translucent granule cell region. Illumination under bright-field conditions with the field diaphragm nearly closed made octopus cells appear bright among dark bundles of myelinated fibers. On breaking in to an octopus cell, its characteristic responses to injected current were used to confirm the visual identification (Bal and Oertel 2000; Golding et al. 1995, 1999).

All measurements of potassium currents were made under conditions in which they could be isolated from other currents. The control solution contained (in mM) 138 NaCl, 4.2 KCl, 2.4 $CaCl_2$, 1.3 $MgCl_2$, 10 HEPES, and 10 glucose, pH 7.4 when saturated with 100% O_2 . The hyperpolarization-activated current, I_h , was blocked by the extracellular application of 50 nM ZD7288 (Bal and Oertel 2000). Voltage-sensitive sodium current was blocked by 1 μM tetrodotoxin (TTX) (Golding et al. 1999). Voltage-sensitive calcium current was blocked by 0.4 or 0.25 mM $CdCl_2$ in most experiments. Synaptic currents were blocked with 40 μM 6,7-dinitroquinoxaline-2,3-dione (DNQX; Tocris Cookson, Avonmouth, UK). In experiments that concerned the high-threshold K^+ conductance, 50 nM α -dendrotoxin (α -DTX; Alomone Labs, Jerusalem, Israel) was added to the control solution. When TEA was applied, it was substituted for Na^+ . Test solutions were applied to the chamber by redirecting the flow of liquid through a system of tubing and valves. Unless otherwise stated, all chemicals were obtained from Sigma (St. Louis, MO).

Pipettes were generally of low resistance (3–6 M Ω). They were pulled from borosilicate glass (1.2 mm OD). They were filled with a solution that consisted of (in mM) 108 potassium gluconate, 9 HEPES, 9 EGTA, 4.5 $MgCl_2$, 14 phosphocreatinine (tris salt), 4 ATP (Na salt), and 0.3 GTP (tris salt); pH was adjusted to 7.4 with KOH (Forscher and Oxford 1985).

Current- and voltage-clamp recordings were performed with standard whole cell patch-clamp techniques using an Axopatch-200A amplifier. Data were low-pass-filtered at 5–10 kHz. Current and voltage records were sampled at 10–40 kHz and were digitized on-line using a Digidata 1320 interface (Axon Instruments, Foster

City, CA) and fed both to a chart recorder and to an IBM-compatible personal computer for storage and further analyses. Stimulus generation, data acquisition, and off-line analysis of digitized data were done using pClamp software (version 8.03; Axon Instruments). After the formation of high-resistance seals (>1 G Ω), negative pressure was applied to obtain the whole cell configuration. Series resistance varied from 6 to 15 M Ω . All reported results were from recordings in which $\geq 95\%$ of the series resistance could be compensated on-line; no corrections were made for errors in voltage that resulted from uncompensated series resistance. In these experiments, the actual voltage was maximally 6 mV less positive than stated. All voltage measurements have been compensated for a junction potential of -12 mV.

Statistical analyses were performed off-line. The results are given as means \pm SD, with n being the number of cells in which the measurement was made. Significant differences between the groups were evaluated using a paired Student's t -test.

RESULTS

Data reported here were obtained from recordings of 153 octopus cells, each lasting between 20 min and 2 h. All reported measurements were made while the hyperpolarization-activated current was blocked by 50 nM ZD7288, voltage-sensitive Na^+ currents were blocked by with 1 μM TTX, and excitatory synaptic currents were blocked by 40 μM DNQX. In most experiments, 0.4 mM Cd^{2+} was added to block Ca^{2+} currents. Inhibitory synaptic currents have not been observed in octopus cells (Gardner et al. 1999; Golding et al. 1995).

Definition of I_{KL} and I_{KH}

Depolarizing voltage steps from a holding potential of -90 mV evoked large outward currents. The threshold for the appearance of voltage-sensitive outward current was -70 mV. The current increased steeply in amplitude with steps to more depolarized potentials and then decayed with relatively slow time course to a steady-state value that was 23% of the peak (Fig. 1A). In the absence of pharmacological blocking agents, the peak outward currents saturated the amplifier at voltages more depolarized than -40 mV. The activation of the outward current was rapid so that its beginning was superimposed on the capacitative current and could not be resolved reliably. Voltage steps from -90 to -40 mV evoked currents that took 1.7 ± 0.2 ms ($n = 6$) to reach half-peak amplitude. To characterize the large, voltage-sensitive outward current in octopus cells required that the components be isolated and identified.

Previous experiments in current clamp have shown that octopus cells have voltage-sensitive Ca^{2+} currents (Golding et al. 1999). The question arose therefore to what extent voltage-sensitive Ca^{2+} currents and Ca^{2+} -activated K^+ currents contribute to the outward current. When external Ca^{2+} was replaced with Mg^{2+} or 0.25 mM Cd^{2+} was added to the bath, the amplitude and the shape of outward current evoked by pulses up to -40 mV did not change measurably (data not shown). Over the voltage range -90 to -40 mV under the present conditions, therefore Ca^{2+} and Ca^{2+} -activated K currents are negligible.

Blockers of K^+ channels blocked most of the outward current and provided an initial separation and identification of the currents. α -DTX blocked a low-threshold current, leaving a high-threshold current that was sensitive to TEA. α -DTX has

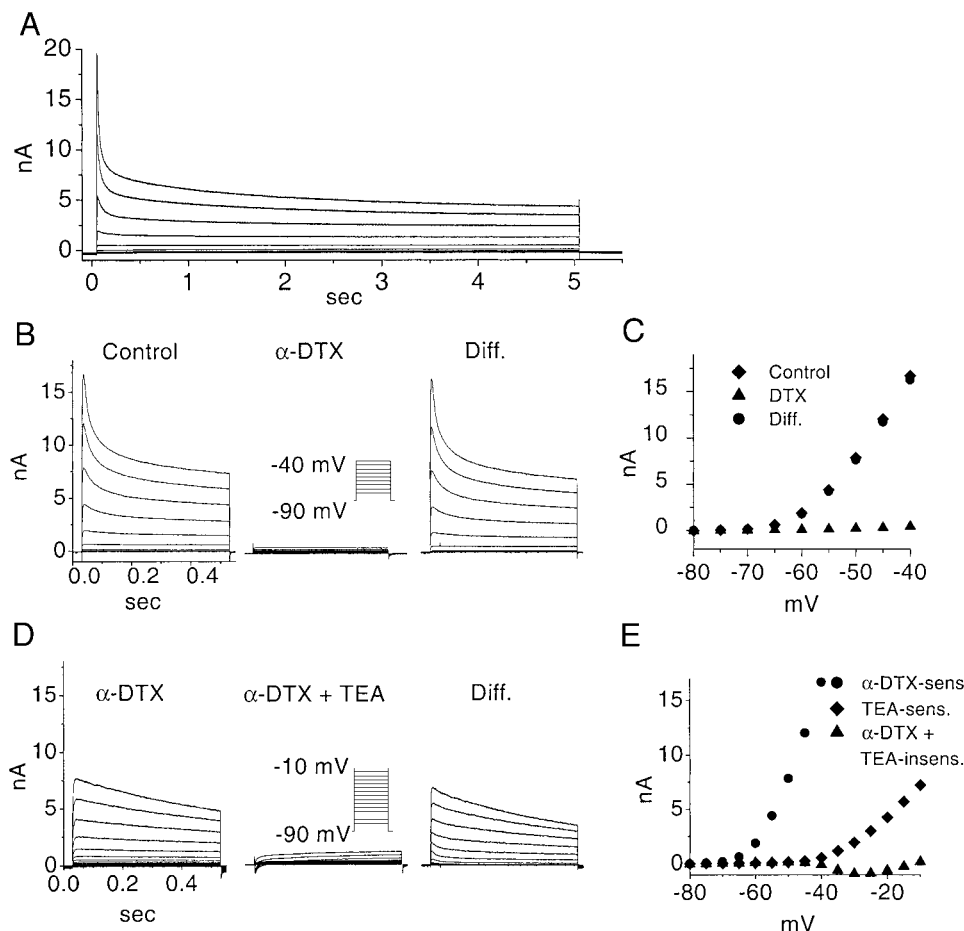


FIG. 1. Octopus cells have pharmacologically distinct low-threshold (I_{KL}) and high-threshold (I_{KH}), voltage-sensitive outward currents. *A*: long, depolarizing voltage steps evoked a transient outward current that inactivated quickly but only partially. From a holding potential of -90 mV, voltage pulses were stepped from -80 to -40 mV in 5 -mV steps. *B*: currents evoked by similar but shorter voltage steps illustrate how I_{KL} was isolated. The currents in the middle panel, measured in the presence of 50 nM α -DTX, were subtracted from those in the left panel recorded under control conditions. *Right*: the difference currents, the α -DTX-sensitive current. *C*: current-voltage relationships of the peak whole cell currents in control saline (\blacklozenge), in the presence of α -DTX (\blacktriangle), and the difference currents (\bullet). *D*: in the same cell and in the continued presence of 50 nM α -DTX, depolarizing steps between -80 and -10 mV evoked outward currents with higher thresholds (*left*). These currents were largely blocked by 10 mM TEA (*middle*). The difference currents (*right*) represent the TEA-sensitive, I_{KL} . *E*: *I-V* relationships of the peaks of α -DTX-sensitive currents, I_{KL} (\bullet), TEA-sensitive- α -DTX insensitive currents I_{KH} (\blacklozenge), and the residual currents (\blacktriangle) are shown. The currents were recorded in the presence of 1 μ M TTX, 50 nM ZD7288 and 40 μ M M DNQX (but not extracellular Cd^{2+}).

been shown to be a selective blocker for low-threshold K^+ outward currents in other types of neurons (Brew and Forsythe 1995; Gamkrelidze et al. 1998; Halliwell et al. 1986; Harvey 1997; Owen et al. 1997; Reid et al. 1999; Southan and Robertson 2000). Figure 1*B* shows that α -DTX blocked 96% of the outward current over the voltage range between about -70 and -40 mV. This experiment shows that the identical current can be isolated on the basis of its voltage sensitivity and on the basis of its pharmacological sensitivity to α -DTX and serves as a test for the specificity of α -DTX. The α -DTX-sensitive current had a low threshold of activation, about -70 mV, serving as the basis for our referring to this current as the low-threshold potassium current, I_{KL} . Its activation was rapid, requiring on average 1.7 ms to reach the half-peak amplitude. Over ~ 0.5 s, this current inactivated to $\sim 50\%$. As octopus cells have resting potentials near -62 mV (Bal and Oertel 2000; Golding et al. 1995, 1999), this current is partially activated when octopus cells are at rest. In the presence of 50 nM α -DTX, the voltage of octopus cells could be stepped to more depolarized potentials and revealed another outward current with a higher threshold that was sensitive to 20 mM TEA (Fig. 1*D*). This current had a threshold of activation at about -40 mV and is thus termed the high-threshold potassium current, I_{KH} (Fig. 1, *D* and *E*). Voltage steps from -90 to -10 mV evoked a current whose activation was partly obscured by the capacitive current; it rose to half-peak-amplitude in 1.5 ms. This current inactivated more slowly than the α -DTX-sensitive current.

Pharmacological experiments showed that 4-AP and TEA did not discriminate between I_{KL} and I_{KH} . While 5 mM 4-AP blocked I_{KL} , it also decreased the amplitude of I_{KH} . The effects of TEA on I_{KL} were investigated in five octopus cells. TEA, at 10 – 20 mM, reduced the peak amplitude of I_{KL} by between 30 and 40% (data not shown).

Sensitivity to blockers of Kv1 channels

The finding that I_{KL} was sensitive to α -DTX suggested that this current was mediated through ion channels of the Kv1 family (Harvey 1997; Hopkins 1998; Hopkins et al. 1994; Owen et al. 1997; Stühmer et al. 1989). A more detailed study was therefore undertaken of the sensitivity of I_{KL} to α -DTX and other toxins reported to be specific for Kv1 channels. α -DTX is derived from the venom of the green mamba snake. Tests of the specificity of this toxin on homomeric channels in expression systems show that α -DTX is relatively unselective among the various Kv1 homomers. It blocks Kv1.2 channels with somewhat higher affinity than Kv1.1, Kv1.3, and Kv1.6 channels (Dolly and Parcej 1996; Grissmer et al. 1994; Harvey 1997; Owen et al. 1997; Tytgat et al. 1995). DTX-K is derived from the venom of black mamba snakes and is a blocker relatively more specific for Kv1.1 homomeric channels (Owen et al. 1997; Robertson et al. 1996; Wang et al. 1999a,b). Tityustoxin $K\alpha$, derived from the venom of scorpions, is reported to be specific for homomeric channels that contain the Kv1.2 α subunits (Hopkins 1998; Werkman et al. 1993). The

actions of these blockers on heteromeric channels is less well characterized (Hopkins 1998; Hopkins et al. 1994; Tytgat et al. 1995). In some combinations of α subunits, sensitivity to the toxins seems to be conferred by a single toxin-sensitive subunit while in other combinations of subunits sensitivity depends on all four α subunits (Hopkins 1998).

A comparison of the sensitivity of I_{KL} to the less selective Kv1 channel blocker (α -DTX) and the more selective blockers of Kv1.1 (DTX-K) and Kv1.2 (tityustoxin) is shown in Fig. 2. α -DTX (50 nM) blocked 90% of the peak outward current (Fig. 2A); the unblocked current had a high activation threshold (Fig. 2B), indicating that it represented mainly I_{KH} . 40 nM DTX-K blocked maximally 78% and tityustoxin maximally 58% of the outward current. The unblocked portions of the current had low activation thresholds, indicating that each of these toxins blocked only part of I_{KL} (Fig. 2, D and F). Dose-response curves (Fig. 2G) show that the concentrations of all toxins used in the experiments illustrated in Fig. 2, A–F, are at saturating levels. Half-maximal blocking concentrations were 5, 10, and 3 nM for α -DTX, DTX-K, and tityustoxin, respectively. The effects of these toxins were irreversible. These results support the conclusion that I_{KL} is mediated through K^+ channels of the Kv1 family. These findings indicate that I_{KL} in octopus cells is generated through a heterogeneous population of Kv1 channels. About 20% lack Kv1.1 and ~45% lack Kv1.2.

Reversal potential of I_{KL}

The reversal potential of I_{KL} was measured from the tail currents obtained with a conventional double-pulse protocol. The tail currents were evoked by repolarizing to a range of potentials between -62 and -102 mV after a depolarizing pulse to -50 mV for 15 ms (Fig. 3A). The reversal potential was measured in saline that contained 10 mM TEA, 1 μ M TTX, 0.25 mM Cd^{2+} , and 50 nM ZD7288 to suppress other voltage-sensitive currents, I_{KH} , I_{Na} , I_{Ca} , and I_h . The amplitude of the tail current was plotted as a function of the step potential (Fig. 3B). At a normal potassium concentration of 4.2 mM, the current reversed at -75.6 ± 3.8 mV ($n = 20$). The dependence of the reversal potential on the extracellular K^+ concentration was determined by repeating the experiment in saline in which KCl was substituted for equimolar NaCl to give final K^+ concentrations of 17 and 34 mM. Figure 3C shows that the reversal potential of I_{KL} roughly obeys the Nernst relationship for K^+ , confirming the conclusion that I_{KL} is largely carried by K^+ .

The measurement of the reversal potential of I_{KL} deviated somewhat from the theoretical potassium equilibrium potential. The I - V relationship in Fig. 3B deviates from linearity over the voltage range negative to the reversal potential. Also the dependence of the reversal potential on the extracellular K^+ concentration deviated from the Nernst relationship at negative potentials; at 4.2 mM $[K^+]_o$ the measured reversal potential was -76 mV, whereas the equilibrium potential for K^+ was -85 mV. There are several possible explanations and interpretations for these deviations. First, the magnitude of the tail current was measured 0.7 ms after the onset of the second step to avoid possible artifacts from the transient capacitive current, but over such a time period the tail currents can be distorted. A voltage dependence of the decay of tail currents

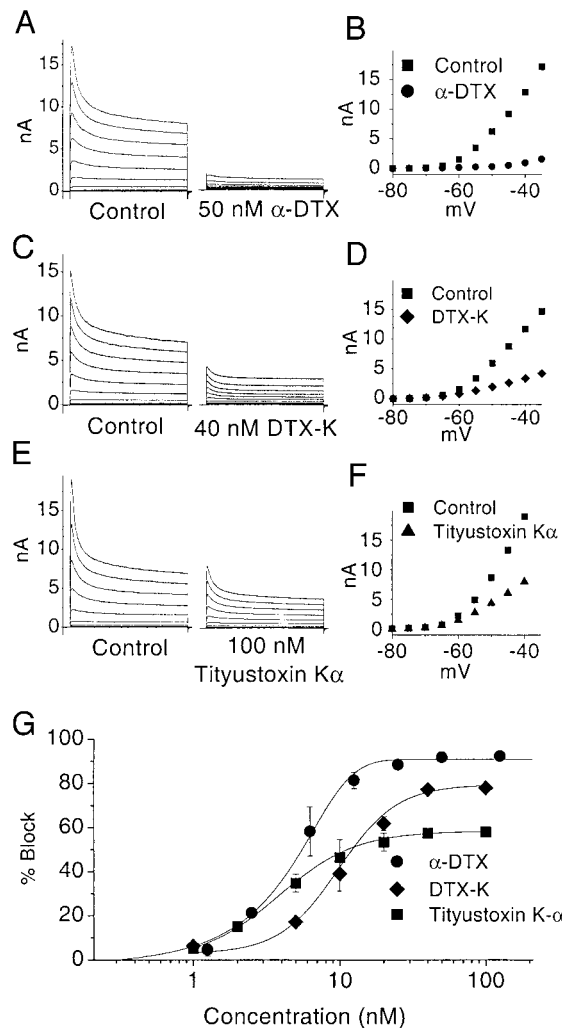


FIG. 2. I_{KL} is sensitive to α -dendrotoxin (α -DTX), DTX-K, and tityustoxin K- α , specific blockers of Kv1 potassium channels. The effects of toxins were assayed in separate cells by measuring to what extent they blocked the peak outward current in response to step depolarizations of 500-ms duration to between -80 mV and -35 or -40 mV from a -90 -mV holding potential. A: α -DTX blocked ~91% of the peak outward current. B: the current-voltage relationships of peak outward currents in the absence (■) and presence (●) of α -DTX are shown for the recording given in A. Most of the unblocked portion of the current activated at high-threshold. C: DTX-K blocked 67% of the peak outward current in this neuron. D: the current-voltage relationships for the recording in C show that the unblocked portion of the current had a low activation threshold. E: tityustoxin K α blocked 58% of the peak outward current. F: the current-voltage relationships for the recording given in E. The unblocked portion of the current had a low activation threshold. G: dose-response relationships for α -DTX ($n = 6$), DTX-K ($n = 3$), and tityustoxin K- α ($n = 3$). Block of I_{KL} is expressed as the percent ratio of peak amplitude in the presence of the blocker to peak amplitude in the absence of the blocker measured in response to voltage steps to -40 mV.

can cause a relative underestimation of the tail currents in the negative voltage range where they decline most rapidly. Second, it is also possible that the outward current might have been contaminated with I_h , a current that is strongly activated at hyperpolarized voltages and that may not have been blocked completely by ZD7288 (Bal and Oertel 2000). Third, it is likely that not all parts of the octopus cell were equally well clamped under all conditions. Fourth, it is possible that I_{KL} is not absolutely specific for K^+ . Fifth, similar deviations in measurements of the reversal potential in avian auditory neurons

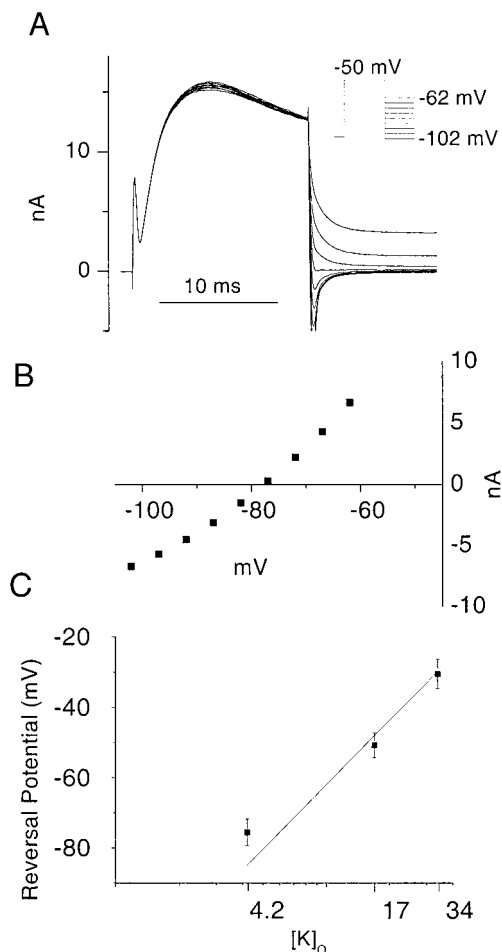


FIG. 3. Measurement of the reversal potential of I_{KL} in whole cell recordings. *A*: tail currents were measured with a double-pulse protocol. These measurements, made in the presence of 4.2 mM extracellular K^+ , indicated that the tail currents reversed near -77 mV. *B*: instantaneous current-voltage (I - V) relationship for the data in *A* measured 0.7 ms after the step change in voltage. The tail currents reversed near -77 mV. *C*: the dependence of reversal potential on extracellular K^+ concentration. The points are means from multiple experiments: $[K^+]_o = 4.2$ mM ($n = 20$), $[K^+]_o = 17$ mM ($n = 4$), and $[K^+]_o = 34$ mM ($n = 4$).

have been attributed to the extracellular accumulation of K^+ (Rathouz and Trussell 1998). Several of these possibilities were assessed in separate experiments.

The reversal potential was measured in recordings in the cell-attached configuration from cell bodies using similar voltage protocols (Fig. 4). In these experiments, the intracellular content was not disturbed, currents are not affected by imperfections in the space-clamp, and there is unlikely to be any extracellular accumulation of K^+ . Recordings were made with pipettes that contained extracellular saline with 50 nM ZD7288, 1 μ M TTX, 10 mM TEA, and 0.25 mM Cd^{2+} . At the end of the recordings, the resting potential was measured in the whole cell mode. The mean reversal potential measured in these experiments was -77 ± 3 mV ($n = 3$), a value that corresponded closely to the reversal potential measured in the whole-cell configuration. The nonlinear I - V relationship of the tail currents under these conditions indicates that neither space-clamping nor K^+ accumulation were the cause of the distortions of the measurements under whole cell conditions.

The possibility that space-clamp artifacts or K^+ accumulation affected measurements of the reversal potential of I_{KL} was tested further by measuring the reversal potential of outward currents in outside-out patches. In these measurements, the reversal potential under normal conditions was found to be -74 ± 2 mV ($n = 3$, data not shown), a value close to that measured in whole cell recordings and deviating from the equilibrium potential of -85 mV.

The most likely explanation for the deviation from theoretical behavior is that the presence of some residual I_h contaminates measurements of the reversal potential at negative potentials. I_h in octopus cells has a threshold of activation between -35 and -40 mV and is strongly activated at more hyperpolarized potentials (Bal and Oertel 2000). The current is small near its reversal potential, -38 mV, where deviations of the reversal potential of I_{KL} from E_K are small, and it is large at more hyperpolarized potentials where the driving force is larger and the conductance is more strongly activated. If 50 nM ZD7288 blocked 91% of a current measured to be between 1 and 2 nA at rest, the resting g_h would be expected to contribute between ~ 0.1 and 0.2 nA at the resting potential and between 0.2 and 0.4 nA at -110 mV.

Voltage sensitivity of the activation of I_{KL}

The potassium currents measured in whole cell recordings of octopus cells are large, requiring additional manipulations to measure the voltage sensitivity of g_{KL} over the physiological range. Steps from -90 to -35 mV often evoked currents that exceeded 20 nA, not only exceeding the limits of the amplifier but also subjecting the measured currents to distortion by the series resistance. To overcome these technical problems, low concentrations of α -DTX were used to reduce peak currents to workable levels. In these experiments, I_{KL} was evoked with steps to -45 mV, then between 5 and 8 nM α -DTX was applied. The ratio of the peak current in the presence and absence of α -DTX indicated what fraction of I_{KL} was blocked by the low concentration of α -DTX and determined the correction factor of g_{KL} in the following measurement. The dif-

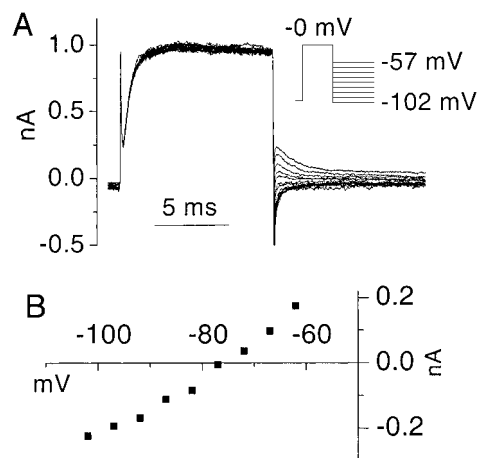


FIG. 4. Measurement of the reversal potential in the cell-attached configuration with a pipette that contained normal extracellular saline with 4.2 mM K^+ , as well as 50 nM ZD7288, 1 μ M TTX, 0.25 mM Cd^{2+} , and 10 mM TEA⁺ which had been substituted for Na^+ . *A*: the tail currents for I_{KL} were measured with a voltage protocol shown in the inset. *B*: I - V relationship for the data in *A*. The tail currents reversed at about -78 mV.

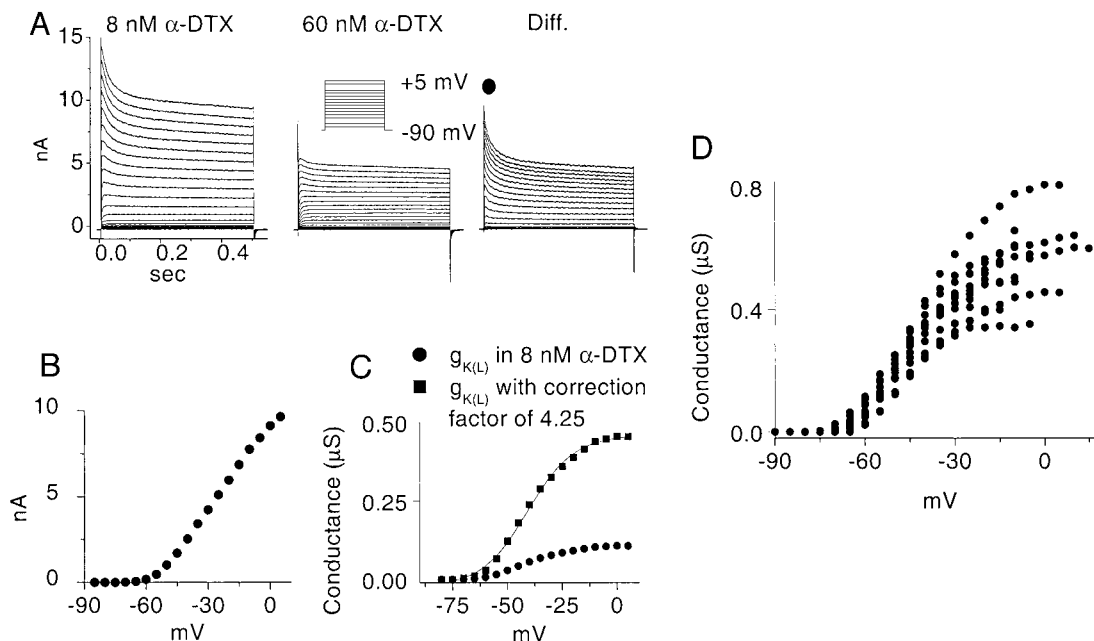


FIG. 5. Voltage dependence of g_{KL} activation. *A*: the current traces were evoked with a voltage protocol given in the *inset*. *Left*: I_{KL} was reduced to measurable amplitudes by 8 nM α -DTX, which reduced the peak outward current at -40 mV by 76.5%. *Middle*: 60 nM α -DTX blocked I_{KL} , leaving I_{KH} and the leak currents. *Right*: the difference between the currents in the *left* and *middle* panels reveals I_{KL} , reduced to 23.5%, over a wide voltage range. *B*: plot of the partially blocked I_{KL} as a function of the voltage. *C*: the conductance derived from the currents in *B*, g_{KL} , without (\bullet) and with (\blacksquare) the application of a correction factor 4.25. The corrected relationship was fitted with a Boltzmann equation, showing that g_{KL} was half-activated at -41 mV and had a slope factor, k of 10 mV. *D*: the relationships of corrected conductance as a function of voltage for 11 experiments show that thresholds are consistently around -70 mV and that the maximum conductance varied among octopus cells.

ference between currents measured in low and high (60 nM) concentrations of α -DTX could then be used to reveal the voltage sensitivity of the unblocked portion of g_{KL} . The results of these experiments are illustrated in Fig. 5. In the presence of 8 nM α -DTX, the outward current evoked by a step to -45 mV was reduced by 76.5% (not shown) and outward currents evoked by depolarizing steps to 0 mV could be measured (Fig. 5A). I_{KL} rises steeply in the voltage range near the resting potential as both the conductance and the driving force increase (Fig. 5B). The voltage sensitivity of g_{KL} was derived from the relationship $g_{KL} = I_{KL}/(V_m - E_K)$. The total g_{KL} was derived by applying a correction factor based on the measurement of the proportion of I_{KL} blocked by a low concentration of α -DTX (Fig. 5C).

The voltage sensitivity of g_{KL} in a group of octopus cells is presented in Fig. 5D. The conductance, g_{KL} , has a threshold near -70 mV, rises steeply in the voltage range near the resting potential and reaches a maximum ~ 0 mV. The sigmoidal relationship can be fit by a Boltzmann function. This analysis indicates that g_{KL} is half-activated at -45 ± 6 mV ($n = 12$) and has a slope factor of 9 ± 2 mV ($n = 12$). The mean maximum g_{KL} for measured in 12 octopus cells was 514 ± 135 nS.

Inactivation of I_{KL}

The decline in I_{KL} in the presence of continuing depolarization indicates that I_{KL} inactivates. The decay of current associated with inactivation in Fig. 1A can best be described by double exponentials of roughly equal weight with time constants in the range of 200 and 20 ms. Knowing that g_{KL} is

activated at rest in the steady state and that this activation is functionally significant, the rate and voltage dependence of inactivation was studied in 11 neurons. After the membrane was conditioned for 1 s to holding potentials between -40 and -105 mV in 5-mV steps, the neuron was depolarized to a fixed test potential, -45 mV (Fig. 6A). The normalized peak current amplitudes were plotted as a function of holding membrane potentials (Fig. 6B). In octopus cells, g_{KL} does not inactivate completely even at very depolarized potentials. The voltage dependence of g_{KL} was fit by a Boltzmann function with $V_{1/2}$ and k values are 64 ± 3 and 5 ± 0.6 mV, respectively ($n = 11$). Near the resting potential, -62 mV, $\sim 40\%$ of the g_{KL} is inactivated; inactivation was maximal at voltages more depolarized than -50 mV.

Measurement of activation and inactivation allows an estimate to be made of the current that is mediated through g_{KL} at rest. At -62 mV, g_{KL} would be expected to have a peak activation of ~ 70 nS. Inactivation would be expected to reduce this conductance by 40% to 42 nS. At the resting potential and under normal ionic conditions, therefore g_{KL} is expected to mediate a current of ~ 1 nA.

Recovery from inactivation of I_{KL}

Recovery from inactivation of I_{KL} depended on the duration and voltage of the recovery period. Inactivation was assayed with a test pulse that followed a conditioning pulse after various intervals. Figure 7A illustrates the results of one such experiment. The cell was held at -100 mV to remove inactivation of I_{KL} completely (Fig. 6B). A depolarizing pulse to -45 mV was used initially to activate and inactivate I_{KL} . A

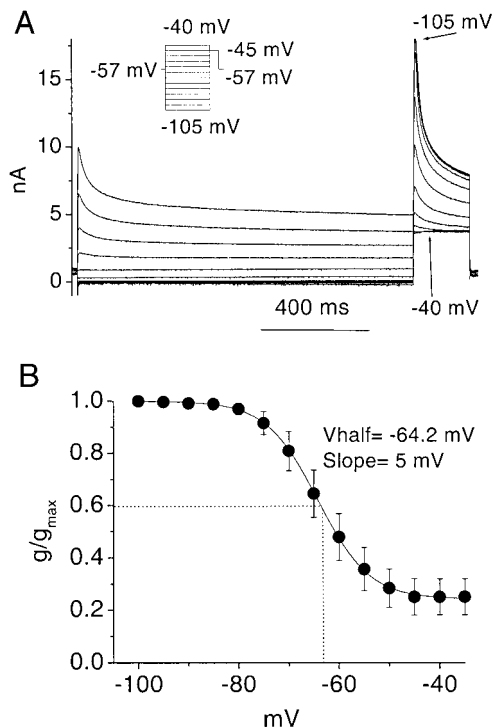


FIG. 6. Voltage dependence of I_{KL} steady-state inactivation. *A*: the currents were evoked by the 2-pulse voltage protocol shown in the inset. Tail currents in the second voltage step to -45 mV reflected activation and inactivation of g_{KL} by the previous voltage step of long enough duration to reach a steady state. *B*: plot of the peaks of tail currents as a function of the voltage of the previous step reveals the voltage dependence of steady-state inactivation. The plot was fit by a Boltzmann function with $V_{1/2}$ at -64.2 ± 2.7 mV and a slope of 5 ± 0.6 mV ($n = 11$).

similar test pulse after intervals that varied between 10 and 2,000 ms at -100 mV was used to assess inactivation. Recovery proceeded with an exponential time course whose time constant was 118 ± 14 ms ($n = 4$) with a complete recovery after ~ 300 ms (Fig. 7*B*). The time constant of recovery depended on the voltage of the recovery period, ranging between about 100 ms at -100 -mV holding potentials and 150 ms near the resting potential (Fig. 7*C*).

Voltage sensitivity of I_{KH}

The high-threshold outward current, I_{KH} , was defined by its insensitivity to α -DTX and its sensitivity to 20 mM TEA. Figure 8 illustrates the properties of this current. Using a bathing saline that contained 50 nM α -DTX, 1 μ M TTX, 0.25 mM Cd^{2+} and 50 nM ZD7288 to suppress I_{KL} , I_{Na} , I_{Ca} and I_h , α -DTX-insensitive outward currents were evoked by voltage steps from a holding potential of -90 mV (Fig. 8*A*, left). In the presence of 20 mM TEA, those outward currents were reduced (Fig. 8*A*, middle) (experiments that are not illustrated showed that $\sim 30\%$ of the remaining outward current could be blocked by 5 mM 4-AP). The difference between these families of currents revealed the TEA sensitive, α -DTX-insensitive current that we define as I_{KH} . As the block of I_{KH} by 20 mM TEA is probably not complete, the amplitude of I_{KH} is underestimated with this method of separating currents. This current has a threshold of activation near -40 mV (Fig. 8*B*). The voltage sensitivity of the underlying conductance was examined by converting current to conductance using Ohm's Law and plot-

ting conductance as a function of voltage (Fig. 8*C*). The relationship was sigmoidal, having a threshold for activation at about -40 mV and saturating at around $+30$ mV. The peak g_{KL} as a function of voltage was described by a Boltzmann function with $V_{1/2}$ at -16 ± 5 mV ($n = 7$) and a slope factor of 10 ± 4 mV ($n = 7$). The maximum conductance, g_{KHmax} was 116 ± 27 nS ($n = 7$). Long depolarizing pulses reveal that I_{KH} inactivated by $\sim 85\%$ (Fig. 8*D*).

Reversal potential of I_{KH}

The reversal potential of I_{KH} was measured with a similar voltage protocol as that described for I_{KL} (Fig. 9*A*). In control saline, the tail current for I_{KH} reversed at -76 ± 4 mV ($n = 6$; Fig. 9*B*), a value within 1 mV of the reversal potential measured for I_{KL} . The finding that the deviation from the equilibrium potential for K^+ of both I_{KL} and I_{KH} are similar argues that a common factor influences both. The results are consistent with I_h affecting measurements of the reversal potential when the reversal potential is in the hyperpolarizing voltage range.

Inactivation of I_{KH}

In the presence of 50 nM α -DTX, a long voltage step to variable voltages activated I_{KH} . The decay of current with continued depolarization shows that I_{KH} inactivates. Inactivation of I_{KH} was slow (Fig. 8*D*); its decay followed a double exponential time course with a dominant (85%) time constant in the range of 500 ms and a second in the range of 25 ms.

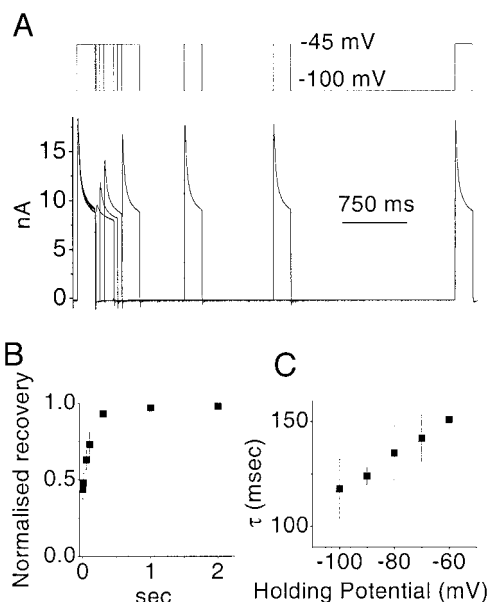


FIG. 7. Recovery of I_{KL} from inactivation is time and voltage dependent. *A*: I_{KL} was evoked by a depolarizing voltage pulse to -45 mV for 200 ms from a holding potential -100 mV and then depolarized to the same potential after various intervals, 10, 50, 100, 300, 1,000, 2,000, and 4,000 ms. *Top*: the voltage protocol; *bottom*: 7 superimposed current records. The current traces were recorded from a single neuron in saline containing 0.25 mM Cd^{2+} , 1 μ M TTX, and 10 mM TEA. *B*: normalized peak current amplitudes were plotted as a function of the interpulse interval. The time course of the recovery, extracted by fitting a single exponential to this relationship was 118 ± 14 ms ($n = 4$). *C*: time course of the recovery differed as a function of holding potential. Time constants of recovery from inactivation are plotted as a function of holding potential.

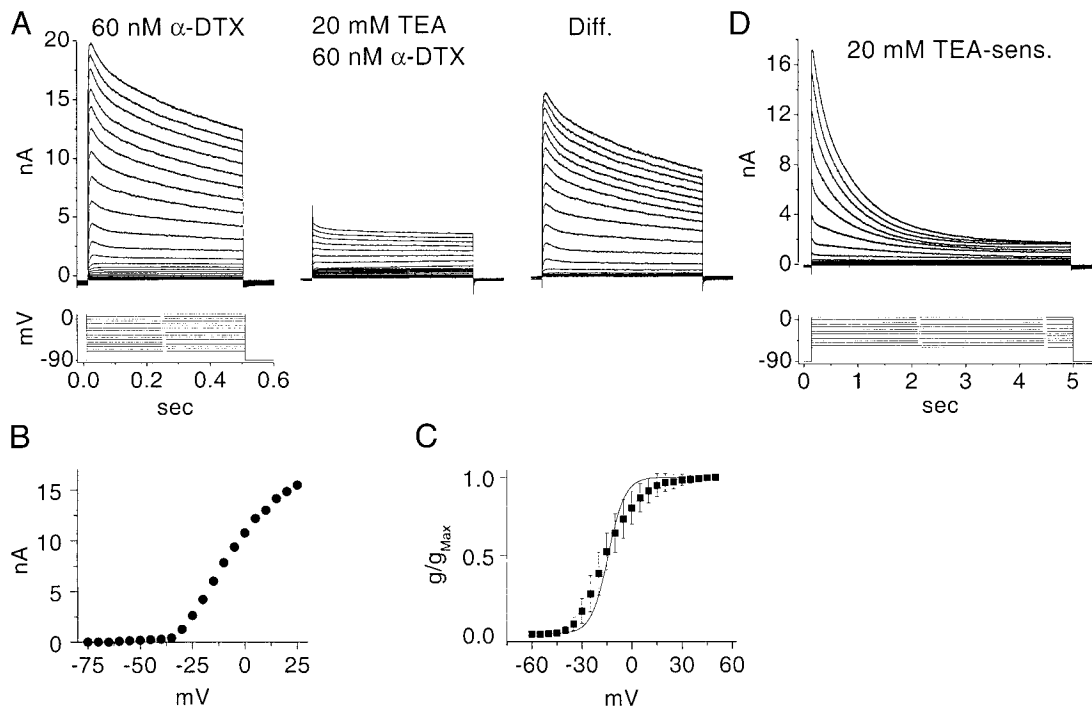


FIG. 8. Voltage sensitivity of I_{KH} and g_{KH} . *A*: currents were evoked with depolarizing steps from a holding potential of -90 mV in the presence of $1 \mu\text{M}$ TTX, 0.25 mM Cd^{2+} , 50 nM ZD7288, and 60 nM $\alpha\text{-DTX}$ to suppress I_{Na} , I_{Ca} , I_h , and I_{KL} , respectively. *Left*: family of currents was evoked when I_{KL} was blocked by $\alpha\text{-DTX}$. *Middle*: similar family of currents evoked in the additional presence of 20 mM TEA. *Right*: difference of currents at the left and middle reveals the TEA-sensitive current. *B*: voltage dependence of the peak I_{KH} was plotted as a function of the step potential with which it was evoked. *C*: the current values were converted into conductance, g_{KL} (\bullet), and normalized. This plot was fit with a Boltzmann function with a half-activation voltage at $-16 \pm 5 \text{ mV}$ ($n = 7$) and a slope factor of $10 \pm 4 \text{ mV}$ ($n = 7$). *D*: the family of I_{KH} recorded ~ 5 s shows that in the steady-state I_{KH} inactivated by $\sim 85\%$.

Figure 10 shows an experiment in which variable voltage steps of 1.5 s were applied; inactivation did not reach a steady state over this time period but octopus cells tended not to tolerate longer depolarizations. Inactivation was assayed with a

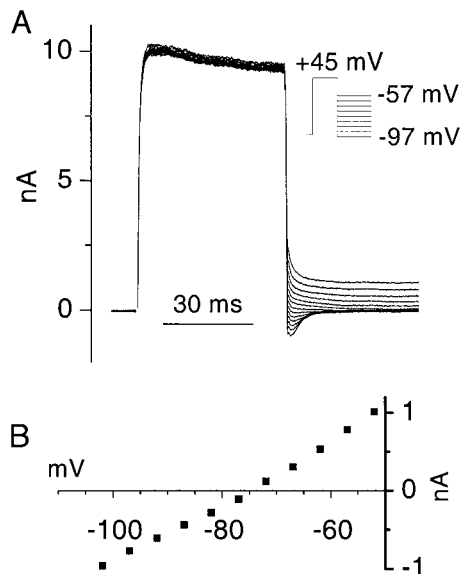


FIG. 9. Measurement of the reversal potential for I_{KH} with whole cell recording. *A*: currents were evoked with a depolarizing voltage step to $+45$ mV. Tail currents were recorded during subsequent steps to various voltages in the presence of 4.2 mM K^+ . *B*: current-voltage relationship for the tail currents in *A* shows that the tail currents reversed near -75 mV .

subsequent voltage step to $+45 \text{ mV}$. The peaks of responses to the test pulse varied as a function of the level of the previous depolarization. A plot of the conductance, derived from the peak tail currents, as a function of the previous voltage step shows a sigmoidal shape that can be fit with a Boltzmann function. The $V_{1/2}$ and slope factor values are 54 ± 6 and 10 ± 2 ($n = 6$) mV, respectively. The fact that inactivation did not reach steady state means that the maximal inactivation was underestimated; Fig. 10*B* shows maximal inactivation to be 75% whereas it can reach 85% .

Contribution of K^+ currents to membrane excitability

To gain an appreciation for the biological consequences of these conductances on octopus cells, the effects of $\alpha\text{-DTX}$, 4-AP and TEA on firing properties of octopus cells were examined in current-clamp experiments. The voltage-clamp experiments show that the application of 50 nM $\alpha\text{-DTX}$ blocked I_{KL} almost completely. When $\alpha\text{-DTX}$ was applied in current clamp, octopus cells depolarized and became more excitable (Fig. 11). The input resistance increased from 6.2 ± 2.5 to $20 \pm 6 \text{ M}\Omega$ ($n = 10$), resulting in an increase in the membrane time constant from 0.22 ± 0.04 ($n = 5$) to 1.9 ± 1 ms ($n = 5$; Fig. 11*B*). In the presence of $\alpha\text{-DTX}$, repetitive slow action potentials could be evoked with depolarizing current. The peaks of the first in the train of action potentials occurred later and varied more than under control conditions (Fig. 11*C*). The latencies from the onset of the current pulse to the peaks of action potentials evoked with depolarizing cur-

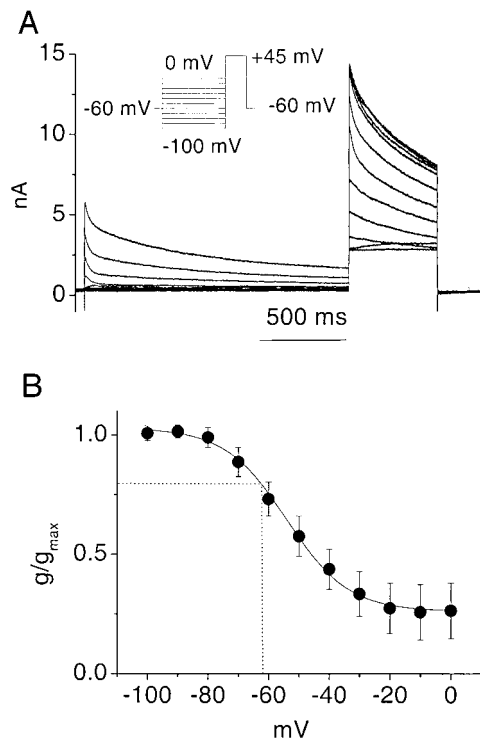


FIG. 10. Voltage dependence of inactivation for I_{KH} . *A*: currents were evoked with a 2-step voltage protocol as shown in the inset. A 1st step to various levels activates I_{KH} to varying degrees and is long enough to allow the current to inactivate. The current traces show that I_{KH} had not quite reached steady state. The 2nd step to a fixed voltage was used to assay inactivation of the current. *B*: conductance was derived from tail currents in responses to the second voltage pulse in 7 cells. The sigmoid relationship was fitted by a Boltzmann function, showing a midpoint at -54 ± 6 mV and a slope of 10 ± 2 mV ($n = 6$).

rents of 1 nA were shifted from 0.58 ± 0.08 ($n = 10$) to 1.8 ± 0.8 ms ($n = 9$) by α -DTX; latencies of action potentials in responses to current pulses of 5 nA changed from 0.35 ± 0.08 ($n = 10$) to 0.69 ± 0.3 ms ($n = 9$). α -DTX also caused a 6.2 ± 2.5 mV depolarizing shift of the resting potential. The subsequent application of 20 mM TEA, which was demonstrated in voltage-clamp experiments to block I_{KH} , eliminated the repetitive firing and allowed octopus cells to be depolarized to a plateau potential that lay positive to 0 mV that was presumably maintained by voltage-sensitive Na^+ and Ca^{2+} currents. These experiments show that g_{KL} contributes to the setting of the resting potential and of the input resistance and time constant of the resting octopus cell. It also shapes the peaks of action potentials and decreases their temporal jitter. As expected, the application of TEA affected only the most depolarized electrophysiological responses, preventing the repolarization of large action potentials (Fig. 11C).

DISCUSSION

This study provides a description of voltage-sensitive K^+ currents, I_{KL} and I_{KH} , and their underlying conductances, g_{KL} and g_{KH} , in octopus cells of the ventral cochlear nucleus. These currents are both identified as K^+ currents by their reversal potentials. The mamba snake toxin, α -DTX, blocks 90% of the K^+ current that is activated at potentials more negative than -45 mV but leaves a K^+ current that was activated at more positive potentials. This toxin was used to separate I_{KL} from I_{KH} in the voltage range where both are activated so that these currents could be studied in isolation. The sensitivity of I_{KL} to the dendrotoxins and to tityustoxin indicates that I_{KL} is probably mediated through voltage-sensitive K^+ channels of the Kv1 family. The high- and low-threshold K^+ conductances

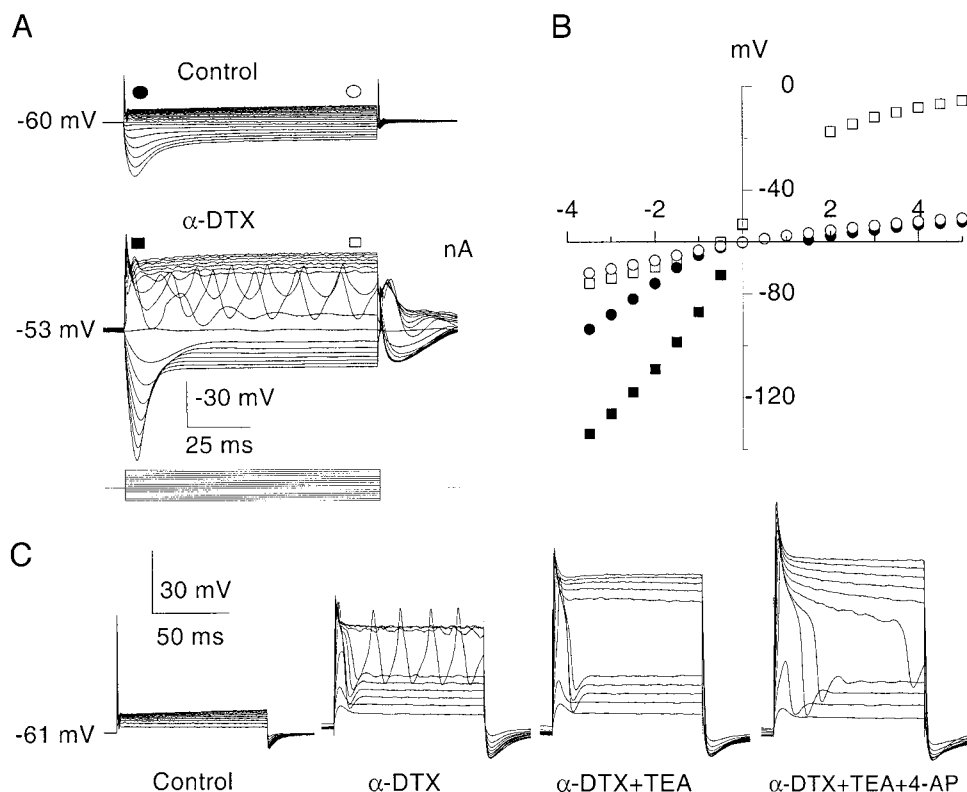


FIG. 11. The role of voltage-sensitive K^+ currents in controlling the resting potential and the excitability of octopus cells. *A*: families of superimposed voltage responses to current pulses. Amplitude of current pulses ranged between -3.5 and 5 nA and were presented in 0.5-nA increments. Application of 50 nM of α -DTX resulted in a depolarizing shift of resting potential and the generation of multiple large, broad action potentials. *B*: voltage-current relationships were plotted before and after application of α -DTX, illustrating that the input resistance of the cell increased. *C*: records from a different octopus cell show that following 50 nM of α -DTX application, the application of 20 mM TEA and 5 mM 4-AP increased the input resistance further. Voltage traces show responses to families of depolarizing current pulses that varied between 0.5 and 5 nA in 0.5-nA increments.

differ in their voltage sensitivity. The threshold of g_{KL} lay at -70 mV, and activation was maximal at voltages positive to 0 mV. This conductance is activated over the entire physiological voltage range of octopus cells. It contributes both to setting the resting potential near -62 mV and to the shaping of responses to synaptic activation through the auditory nerve (Golding et al. 1995). In contrast, the threshold of g_{KH} is at -40 mV and it is maximally activated at $+30$ mV. This conductance affects only the largest, suprathreshold events. It does not affect the resting properties of octopus cells and it does not contribute to the shaping of small synaptic potentials. The biophysical specializations of octopus cells are generated with K^+ conductances whose biophysical and pharmacological properties are conventional but which are represented in octopus cells in unusually large quantities.

I_{KL} and I_{KH} are K^+ currents

Measurements of the reversal potentials for both I_{KL} and I_{KH} deviated from the theoretical equilibrium potential, E_K , when the external concentration of K^+ was low, raising the question whether these currents are always carried by K^+ . Under control conditions, both I_{KL} and I_{KH} reversed at about -76 mV when E_K was -84.5 mV. Similar deviations have been documented in bushy cells of the mammalian cochlear nucleus (Manis and Marx 1991) and their avian homologs (Rathouz and Trussell 1998). When the extracellular K^+ concentration was raised, shifting E_K to more depolarized levels, the reversal potential of g_{KL} matched E_K . The finding that a depolarized reversal potential for I_{KL} was measured also in cell-attached and outside-out configurations indicates that the deviation from the theoretical E_K was not produced by space-clamp errors. Several observations indicate that the deviation from E_K arose from the contamination of K^+ currents with I_h . First, the deviation was similar for both I_{KL} and I_{KH} , indicating that a common factor affected both measurements. Second, the deviation was observed in the voltage range where I_h was activated, and it was not observed outside that voltage range. Third, 50 nM ZD7288 leaves 7% of I_h unblocked (Bal and Oertel 2000); in cells with an unusually large g_h whose voltage range of activation is unusually depolarized, the remaining current is substantial and can account for the deviation. Fourth, deviation was similar in whole cell cell-attached and outside-out patch configurations, arguing against mechanisms that involve depletion or accumulation. We conclude that both I_{KL} and I_{KH} are K^+ currents.

Activation and inactivation of I_{KL} at rest

The observations that g_{KL} is activated at the resting potential and that the maximum g_{KL} is large indicate that g_{KL} contributes substantially to shaping synaptic responses. This conductance had an activation threshold near -70 mV and was half-maximally activated at -45 mV. At rest, -62 mV, a substantial proportion of the mean maximum peak conductance is 514 ± 135 nS, ~ 70 nS, is activated. However, some of that conductance, $\sim 40\%$, will be inactivated, leaving a resting g_{KL} of 42 nS and a resting I_{KL} of ~ 1 nA. This resting K^+ outward current is roughly balanced by an inward current, I_h , which has been estimated to be on average 1.4 nA (between 0.9 and 2.1 nA) (Bal and Oertel 2000; Oertel et al. 2000).

High- and low-threshold K^+ currents in auditory brain stem nuclei

The K^+ conductances in octopus cells bear a striking resemblance to conductances in other auditory neurons. In cochlear nuclear bushy cells and their avian homologs as well as in neurons of the medial nucleus of the trapezoid body, low- and high-threshold K^+ conductances have been described (Brew and Forsythe 1995; Manis and Marx 1991; Rathouz and Trussell 1998; Reyes et al. 1994). While the methods for separation of currents varied, the low-threshold conductances were sensitive to dendrotoxins (Brew and Forsythe 1995; Rathouz and Trussell 1998). In octopus cells, the maximum g_{KL} , 514 ± 135 , is at least six times larger than in any other auditory or nonauditory neurons in which it has been measured. Estimates of the maximum g_{KL} in other auditory neurons are as follows: isolated bushy cells, 15 nS (Manis and Marx 1991); avian nucleus magnocellularis, 68 nS (Rathouz and Trussell 1998); and neurons of the medial nucleus of the trapezoid body, 10 nS (Brew and Forsythe 1995). High-threshold conductances in octopus cells were also larger than in other cells, but the difference was smaller. Comparison of magnitudes of g_{KH} is made difficult by the differences in techniques for defining the high-threshold conductance. In octopus cells, the maximum g_{KH} averaged 116 nS. In neurons of the medial nucleus of the trapezoid body, maximum g_{KH} is roughly 32 nS (Brew and Forsythe 1995). In avian homologs of bushy cells, it was 44 nS (Rathouz and Trussell 1998). Roughly the total maximal g_K in octopus cells is at least eight times that in other neurons in auditory brain stem (Brew and Forsythe 1995; Manis and Marx 1991; Rathouz and Trussell 1998). The maximal total g_K is 10 – 100 times larger in octopus cells than in nonauditory neurons in the CNS (e.g., Bardoni and Belluzzi 1993; Schofield and Ikeda 1989; Wu and Barish 1992).

Low-threshold K^+ conductances that are sensitive to α -DTX and that belong to the Kv1 family are widespread in the nervous system. They have been shown to play a role in the hippocampus (Halliwell et al. 1986) and in central vestibular neurons (Gamkrelidze et al. 1998). They have been shown to regulate excitability in not only cell bodies but also in axons and axon terminals (Reid et al. 1999; Southan and Robertson 2000; Zhou et al. 1999).

I_{KL} is mediated through K^+ channels of the Kv1 family

Native channels of the Kv1 family are generally thought to comprise four α and four β subunits. Combinations of α subunits form functional homomeric as well as heteromeric channels in vitro, even in the absence of β subunits, indicating that the α subunits form the pore of the channel and control its gating. The β subunits of Kv1 channels in mammalian cells affect the expression and modulate the biophysical properties of the channels (Coleman et al. 1999). Kv β subunits accelerate inactivation and cause a hyperpolarizing shift in the activation curve of Kv1 channels (Accili et al. 1997; Heinemann et al. 1996; Rettig et al. 1994; Uebele et al. 1998).

A group of peptide toxins has recently been developed and characterized that has proven to be specific for channels of the Kv1 family. These peptide toxins include α -DTX, its close homologue DTX-I, DTX-K, δ DTX, and tityustoxin. When tested on homomeric channels in expression systems, α -DTX

and DTX-I potently block Kv1.2 channels, and with lower potency, they also block Kv1.1, Kv1.3, and Kv1.6 channels (Dolly and Parcej 1996; Grissmer et al. 1994; Harvey 1997; Hopkins 1998; Owen et al. 1997; Tytgat et al. 1995). DTX-K specifically blocks Kv1.1 homomers and has little effect on other Kv1 channels (Robertson et al. 1996; Wang et al. 1999a,b). δ DTX blocks Kv1.1 channels with high potency (Hopkins 1998). Tityustoxin has been shown specifically to block homomeric Kv1.2 channels (Hopkins 1998; Werkman et al. 1993). In general these toxins also block heteromers that contain a single subunit for which they are specific (Hopkins 1998; Hopkins et al. 1994; Wang et al. 1999a). There are exceptions, however; the tityustoxin block of Kv1.2/Kv1.4 heteromers does not fit this model (Hopkins 1998).

It is likely that Kv1 channels exist as heteromers in octopus cells. Manganas and Trimmer (2000) suggest that Kv1.1 and Kv1.2 α subunits require coassembly with another member of the Kv1 family, one possibility being Kv1.4, to be expressed at the surface of mammalian cells. Biochemical and immunohistochemical studies confirm this conclusion and indicate that Kv1.1 α subunits form heteromultimers with either Kv1.4 or Kv1.2 or both (Coleman et al. 1999; Koch et al. 1997; Shamotienko et al. 1997). Coexpression of Kv1 subunits in *Xenopus* oocytes resulted in the formation of heterotetrameric channels with pharmacological and biophysical properties distinct from those of corresponding homotetrameric channels subunit (Hopkins 1998; Hopkins et al. 1994; Isacoff et al. 1990; Ruppersberg et al. 1990; Sheng et al. 1993; Tytgat et al. 1995; Wang et al. 1993).

None of the homomeric channel currents of Kv1.1, Kv1.2, and Kv1.4 in vitro expression systems has identical pharmacological and biophysical properties to I_{KL} in octopus cells. Instead, I_{KL} in octopus cells combines the features of homomeric channels. The low threshold of I_{KL} resembles that of Kv1.1 homomeric channels (Grissmer et al. 1994; Hopkins et al. 1994; Stühmer et al. 1989). The rapid inactivation resembles that of Kv1.4 homomeric channels (Dolly and Parcej 1996; Stühmer et al. 1989). The properties of inactivation resemble those of Kv1.1 and Kv1.2 channels (Hopkins et al. 1994).

I_{KL} in octopus cells is likely to be generated through a heterogeneous population of heteromeric channels that contain Kv1.1 and/or Kv1.2 as well as Kv1.4. These subunits are strongly expressed in octopus cells. In situ hybridization shows the expression of mRNA for Kv1.1 and Kv1.2 (Grigg et al. 2000). Immunohistochemical evidence has also revealed the presence of Kv1.1 and Kv1.2 (Wang et al. 1994) and Kv1.4 (Fonseca et al. 1998) proteins in octopus cells. The differential sensitivity of I_{KL} to α -DTX, DTX-K, and tityustoxin suggests that the population of K⁺ channels that mediates I_{KL} is heterogeneous. DTX-K, specific for Kv1.1 channels (Dolly and Parcej 1996; Wang et al. 1999a), blocks maximally 70% of I_{KL}. Tityustoxin blocks maximally ~60% of I_{KL}, indicating that 40% of channels lack Kv1.2 subunits (Hopkins 1998; Werkman et al. 1993). Assuming that a single Kv1.1 or Kv1.2 subunit renders channels sensitive to DTX-K and tityustoxin, respectively, an assumption known not to apply to all combinations of subunits (Hopkins 1998), then ~30% of channels lack Kv1.1 subunits and ~40% lack Kv1.2 subunits.

Octopus cells have β subunits. Fonseca et al. (1998) have observed that the subunits, Kv β 1 and Kv β 2, are abundantly

expressed in octopus cells. β subunits may account partially for the rapid inactivation and hyperpolarized activation threshold of I_{KL}.

Molecular basis for I_{KH} is unknown

I_{KH} is characterized by its high-threshold, -40 mV, by its insensitivity to α -DTX, and by its sensitivity to 20 mM TEA. It is not possible to attribute this current to a particular family of K⁺ channels. Ion channels in the Kv3, or *Shaw*, family generally have high-thresholds and vary in inactivation. Octopus cells have been examined for the presence of mRNA for the Kv3.1 subunit. While the present study shows that g_{KH} is larger in octopus cells than in bushy cells, both mRNA and protein is present at lower levels in octopus than in other cochlear nuclear cells including bushy cells (Grigg et al. 2000; Perney and Kaczmarek 1997).

We owe particular thanks to the staff of Alomone Labs, who were exceptionally helpful in advising us and supplying us with dendrotoxins and tityustoxin. Dr. K. Fujino made thoughtful comments about the manuscript for which we are very grateful. This work benefited from discussions with Drs. S. Gardner and K. Fujino about practical and theoretical details. We also thank I. Siggelkow for help in keeping us supplied with solutions.

This work was supported by National Institute on Deafness and Other Communication Disorders Grant DC-00176.

Present address of R. Bal: Dept. of Physiology, Faculty of Veterinary Medicine, Mustafa Kemal University, Antakya/Hatay, Turkey.

REFERENCES

- ACCILI EA, KIEHN J, YANG Q, WANG Z, BROWN AM, AND WIBLE BA. Separable Kv β subunit domains alter expression and gating of potassium channels. *J Biol Chem* 272: 25824–25831, 1997.
- ADAMS JC. Neuronal morphology in the human cochlear nucleus. *Arch Otolaryngol Head Neck Surg* 112: 1253–1261, 1986.
- ADAMS JC. Projections from octopus cells of the posteroventral cochlear nucleus to the ventral nucleus of the lateral lemniscus in cat and human. *Aud Neurosci* 3: 335–350, 1997.
- BAL R AND OERTEL D. Hyperpolarization-activated, mixed-cation current (I_h) in octopus cells of the mammalian cochlear nucleus. *J Neurophysiol* 84: 806–817, 2000.
- BARDONI R AND BELLUZZI O. Kinetic study and numerical reconstruction of A-type current in granule cells of rat cerebellar slices. *J Neurophysiol* 69: 2222–2231, 1993.
- BRAWER JR, MOREST DK, AND KANE EC. The neuronal architecture of the cochlear nucleus of the cat. *J Comp Neurol* 155: 251–300, 1974.
- BREW HM AND FORSYTHE ID. Two voltage-dependent K⁺ conductances with complementary functions in postsynaptic integration at a central auditory synapse. *J Neurosci* 15: 8011–8022, 1995.
- COLEMAN SK, NEWCOMBE J, PRYKE J, AND DOLLY JO. Subunit composition of Kv1 channels in human CNS. *J Neurochem* 73: 849–858, 1999.
- DOLLY JO AND PARCEJ DN. Molecular properties of voltage-gated K⁺ channels. *J Bioener Biomemb* 28: 231–253, 1996.
- FONSECA RC, HALLOWS JL, TRIMMER JS, RHODES KJ, AND TEMPEL BL. Localization of Kv channels in the auditory system. *Assoc Res Otolaryngol Abstr* 21: 213, 1998.
- FORSCHER P AND OXFORD GS. Modulation of calcium channels by norepinephrine in internally dialyzed avian sensory neurons. *J Gen Physiol* 85: 743–763, 1985.
- FRIAUF E AND OSTWALD J. Divergent projections of physiologically characterized rat ventral cochlear nucleus neurons as shown by intra-axonal injection of horseradish peroxidase. *Exp Brain Res* 73: 263–284, 1988.
- GAMKRELIDZE G, GIAUME C, AND PEUSNER KD. The differential expression of low-threshold sustained potassium current contributes to the distinct firing patterns in embryonic central vestibular neurons. *J Neurosci* 18: 1449–1464, 1998.
- GARDNER SM, TRUSSELL LO, AND OERTEL D. Time course and permeation of synaptic AMPA receptors in cochlear nuclear neurons correlate with input. *J Neurosci* 19: 8721–8729, 1999.

- GODFREY DA, KIANG NYS, AND NORRIS BE. Single unit activity in the posteroventral cochlear nucleus of the cat. *J Comp Neurol* 162: 247–268, 1975.
- GOLDING NL, FERRAGAMO MJ, AND OERTEL D. Role of intrinsic conductances underlying transient responses of octopus cells of the cochlear nucleus. *J Neurosci* 19: 2897–2905, 1999.
- GOLDING NL, ROBERTSON D, AND OERTEL D. Recordings from slices indicate that octopus cells of the cochlear nucleus detect coincident firing of auditory nerve fibers with temporal precision. *J Neurosci* 15: 3138–3153, 1995.
- GRIGG JJ, BREW HM, AND TEMPEL BL. Differential expression of voltage-gated potassium channel genes in auditory nuclei of the mouse brainstem. *Hear Res* 140: 77–90, 2000.
- GRISSMER S, NGUYEN AN, AIYAR J, HANSON DC, MATHER RJ, GUTMAN GA, KARMILOWICZ MJ, AUUPERIN DD, AND CHANDY KG. Pharmacological characterization of five cloned voltage-gated K⁺ channels, types Kv1.1, 1.2, 1.3, 1.5, and 3.1, stably expressed in mammalian cell lines. *Mol Pharmacol* 45: 1227–1234, 1994.
- HACKNEY CM, OSEN KK, AND KOLSTON J. Anatomy of the cochlear nuclear complex of guinea pig. *Anat Embryol (Berl)* 182: 123–149, 1990.
- HALLIWELL JV, OTHMAN IB, PELCHEN-MATTHEWS A, AND DOLLY JO. Central action of dendrotoxin: selective reduction of a transient K conductance in hippocampus and binding to localized acceptors. *Proc Nat Acad Sci USA* 83: 493–497, 1986.
- HARVEY AL. Recent studies on dendrotoxins and potassium ion channels. *Gen Pharmacol* 28: 7–12, 1997.
- HEINEMANN SH, RETTIG J, GRAACK HR, AND PONGS O. Functional characterization of Kv channel beta-subunits from rat brain. *J Physiol (Lond)* 493: 625–633, 1996.
- HOPKINS WF. Toxin and subunit specificity of blocking affinity of three peptide toxins for heteromultimeric, voltage-gated potassium channels expressed in *Xenopus* oocytes. *J Pharmacol Exp Ther* 285: 1051–1060, 1998.
- HOPKINS WF, ALLEN ML, HOUAMED KM, AND TEMPEL BL. Properties of voltage-gated K⁺ currents expressed in *Xenopus* oocytes by mKv1.1, mKv1.2 and their heteromultimers as revealed by mutagenesis of the dendrotoxin-binding site in mKv1.1. *Eur J Physiol* 428: 382–390, 1994.
- ISACOFF EY, JAN YN, AND JAN LY. Evidence for the formation of heteromultimeric potassium channels in *Xenopus* oocytes. *Nature* 345: 530–534, 1990.
- KOCH RO, WANNER SG, KOSCHAK A, HANNER M, SCHWARZER C, KACZOROWSKI GJ, SLAUGHTER RS, GARCIA ML, AND KNAUS HG. Complex subunit assembly of neuronal voltage-gated K⁺ channels. Basis for high-affinity toxin interactions and pharmacology. *J Biol Chem* 272: 27577–27581, 1997.
- KOLSTON J, OSEN KK, HACKNEY CM, OTTERSEN OP, AND STORM-MATHISEN J. An atlas of glycine- and GABA-like immunoreactivity and colocalization in the cochlear nuclear complex of the guinea pig. *Anat Embryol (Berl)* 186: 443–465, 1992.
- KULEZA RJ AND BERREBI AS. Distribution of GAD isoforms in the superior paraolivary nucleus (SPON) of the rat. *Assoc Res Otolaryngol Abstr* 22: 70–71, 1999.
- MANGANAS LN AND TRIMMER JS. Subunit composition determines Kv1 potassium channel surface expression. *J Biol Chem* 275: 29685–29693, 2000.
- MANIS PB AND MARX SO. Outward currents in isolated ventral cochlear nucleus neurons. *J Neurosci* 11: 2865–2880, 1991.
- OERTEL D, BAL R, GARDNER SM, SMITH PH, AND JORIS PX. Detection of synchrony in the activity of auditory nerve fibers by octopus cells of the mammalian cochlear nucleus. *Proc Natl Acad Sci USA* 97: 11773–11779, 2000.
- OERTEL D, WU SH, GARB MW, AND DIZACK C. Morphology and physiology of cells in slice preparations of the posteroventral cochlear nucleus of mice. *J Comp Neurol* 295: 136–154, 1990.
- OSEN KK. Cytoarchitecture of the cochlear nuclei in the cat. *J Comp Neurol* 136: 453–484, 1969.
- OWEN DG, HALL A, STEPHENS G, STOW J, AND ROBERTSON B. The relative potencies of dendrotoxins as blockers of the cloned voltage-gated K⁺ channel, mKv1.1 (MK-1), when stably expressed in Chinese hamster ovary cells. *Br J Pharmacol* 120: 1029–1034, 1997.
- PERNEY TM AND KACZMAREK LK. Localization of a high threshold potassium channel in the rat cochlear nucleus. *J Comp Neurol* 386: 178–202, 1997.
- RATHOUZ M AND TRUSSELL L. Characterization of outward currents in neurons of the avian nucleus magnocellularis. *J Neurophysiol* 80: 2824–2835, 1998.
- REID G, SCHOLZ A, BOSTOCK H, AND VOGEL W. Human axons contain at least five types of voltage-dependent potassium channel. *J Physiol (Lond)* 518: 681–696, 1999.
- RETTIG J, HEINEMANN SH, WUNDER F, LORRA C, PARCEJ DN, DOLLY JO, AND PONGS O. Inactivation properties of voltage-gated K⁺ channels altered by presence of β -subunit. *Nature* 369: 289–294, 1994.
- REYES AD, RUBEL EW, AND SPAIN WJ. Membrane properties underlying the firing of neurons in the avian cochlear nucleus. *J Neurosci* 14: 5352–5364, 1994.
- RHODE WS, OERTEL D, AND SMITH PH. Physiological response properties of cells labeled intracellularly with horseradish peroxidase in cat ventral cochlear nucleus. *J Comp Neurol* 213: 448–463, 1983.
- RHODE WS AND SMITH PH. Encoding timing and intensity in the ventral cochlear nucleus of the cat. *J Neurophysiol* 56: 261–286, 1986.
- ROBERTSON B, OWEN D, STOW J, BUTLER C, AND NEWLAND C. Novel effects of dendrotoxin homologues on subtypes of mammalian Kv1 potassium channels expressed in *Xenopus* oocytes. *FEBS Lett* 383: 26–30, 1996.
- RUPPERSBERG JP, SCHROTER KH, SAKMANN B, STOCKER M, SEWING S, AND PONGS O. Heteromultimeric channels formed by rat brain potassium-channel proteins. *Nature* 345: 535–537, 1990.
- SAINTE MARIE RL, SHNEIDERMAN A, AND STANFORTH DA. Patterns of gamma-aminobutyric acid and glycine immunoreactivities reflect structural and functional differences of the cat lateral lemniscal nuclei. *J Comp Neurol* 389: 264–276, 1997.
- SCHOFIELD BR. Projections from the cochlear nucleus to the superior paraolivary nucleus in guinea pigs. *J Comp Neurol* 360: 135–149, 1995.
- SCHOFIELD BR AND CANT NB. Ventral nucleus of the lateral lemniscus in guinea pigs: cytoarchitecture and inputs from the cochlear nucleus. *J Comp Neurol* 379: 363–385, 1997.
- SCHOFIELD GG AND IKEDA SR. Potassium currents of acutely isolated adult rat superior cervical ganglion neurons. *Brain Res* 485: 205–214, 1989.
- SHAMOTIENKO OG, PARCEJ DN, AND DOLLY JO. Subunit combinations defined for K⁺ channel Kv1 subtypes in synaptic membranes from bovine brain. *Biochemistry* 36: 8195–8201, 1997.
- SHENG M, LIAO YJ, JAN YN, AND JAN LY. Presynaptic A-current based on heteromultimeric K⁺ channels detected in vivo. *Nature* 365: 72–75, 1993.
- SMITH PH, JORIS PX, BANKS MI, AND YIN TCT. Responses of cochlear nucleus cells and projections of their axons. In: *The Mammalian Cochlear Nuclei, Organization and Function*, edited by Merchan MA, Juiz JM, Godfrey DA, and Mugnaini E. New York: Plenum, 1993, p. 349–360.
- SOUTHAN AP AND ROBERTSON B. Electrophysiological characterization of voltage-gated K(+) currents in cerebellar basket and purkinje cells: Kv1 and Kv3 channel subfamilies are present in basket cell nerve terminals. *J Neurosci* 20: 114–122, 2000.
- STÜHMER W, RUPPERSBERG JP, SCHROTER KH, SAKMANN B, STOCKER M, GIESE KP, PERSCHKE A, BAUMANN A, AND PONGS O. Molecular basis of functional diversity of voltage-gated potassium channels in mammalian brain. *EMBO J* 8: 3235–3244, 1989.
- TYTGAT J, DEBONT T, CARMELIET E, AND DAENENS P. The α -dendrotoxin footprint on a mammalian potassium channel. *J Biol Chem* 270: 24776–24781, 1995.
- UEBELE VN, ENGLAND SK, GALLAGHER DJ, SNYDERS DJ, BENNETT PB, AND TAMKUN MM. Distinct domains of the voltage-gated K⁺ channel Kv β 1.3 β -subunit affect voltage-dependent gating. *Am J Physiol Cell Physiol* 274: C1485–C1495, 1998.
- VATER M, COVEY E, AND CASSEDAY JH. The columnar region of the ventral nucleus of the lateral lemniscus in the big brown bat (*Eptesicus fuscus*): synaptic arrangements and structural correlates of feedforward inhibitory function. *Cell Tissue Res* 289: 223–233, 1997.
- WANG FC, BELL N, REID P, SMITH LA, MCINTOSH P, ROBERTSON B, AND DOLLY JO. Identification of residues in dendrotoxin K responsible for its discrimination between neuronal K⁺ channels containing Kv1.1 and 1.2 α subunits. *Eur J Biochem* 263: 222–229, 1999a.
- WANG FC, PARCEJ DN, AND DOLLY JO. α subunit compositions of Kv1.1-containing K⁺ channel subtypes fractionated from rat brain using dendrotoxins. *Eur J Biochem* 263: 230–237, 1999b.
- WANG H, KUNKEL DD, MARTIN TM, SCHWARTZKROIN PA, AND TEMPEL BL. Heteromultimeric K⁺ channels in terminal and juxtaparanodal regions of neurons. *Nature* 365: 75–79, 1993.
- WANG H, KUNKEL DD, SCHWARTZKROIN PA, AND TEMPEL BL. Localization of Kv1.1 and Kv1.2, two K channel proteins, to synaptic terminals, somata, and dendrites in the mouse brain. *J Neurosci* 14: 4588–4599, 1994.
- WARR WB. Fiber degeneration following lesions in the posteroventral cochlear nucleus of the cat. *Exp Neurol* 23: 140–155, 1969.

- WERKMAN TR, GUSTAFSON TA, ROGOWSKI RS, BLAUSTEIN MP, AND ROGAWSKI MA. Tityustoxin-K alpha, a structurally novel and highly potent K^+ channel peptide toxin, interacts with the alpha-dendrotoxin binding site on the cloned Kv1.2 K^+ channel. *Mol Pharmacol* 44: 430–436, 1993.
- WICKESBERG RE, WHITLON DS, AND OERTEL D. In vitro modulation of somatic glycine-like immunoreactivity. *J Comp Neurol* 339: 311–327, 1994.
- WILLARD FH AND MARTIN GF. The auditory brainstem nuclei and some of their projections to the inferior colliculus in the North American opossum. *Neuroscience* 10: 1203–1232, 1983.
- WILLOTT JF AND BROSS LS. Morphology of the octopus cell area of the cochlear nucleus in young and aging C57BL/6J and CBA/J mice. *J Comp Neurol* 300: 61–81, 1990.
- WU RL AND BARISH ME. Two pharmacologically and kinetically distinct transient potassium currents in cultured embryonic mouse hippocampal neurons. *J Neurosci* 12: 2235–2246, 1992.
- ZHOU L, MESSING A, AND CHIU SY. Determinants of excitability at transition zones in Kv1.1-deficient myelinated nerves. *J Neurosci* 19: 5768–5781, 1999.